Received: 17 December 2021 | Accepted: 6 March 2022

DOI: 10.1002/hep4.1942

ORIGINAL ARTICLE

LKB1 acts as a critical brake for the glucagon-mediated fasting response

Suehelay Acevedo-Acevedo | Megan L. Stefkovich | Sun Woo Sophie Kang | Rory P. Cunningham | Constance M. Cultraro | Natalie Porat-Shliom

Thoracic and GI Malignancies Branch, Center for Cancer Research, National Cancer Institute, NIH, Bethesda, Maryland, USA

Correspondence
Natalie Porat-Shliom, Thoracic and GI Malignancies Branch, Center for Cancer Research, National Cancer Institute, Building 10, Room 12C207 MSC 1919, Bethesda, MD 20892, USA.
Email: poratshliomn@mail.nih.gov

Funding information
The Intramural Research Program at the National Institutes of Health, National Cancer Institute (1ZIABC011828)

Abstract

As important as the fasting response is for survival, an inability to shut it down once nutrients become available can lead to exacerbated disease and severe wasting. The liver is central to transitions between feeding and fasting states, with glucagon being a key initiator of the hepatic fasting response. However, the precise mechanisms controlling fasting are not well defined. One potential mediator of these transitions is liver kinase B1 (LKB1), given its role in nutrient sensing. Here, we show LKB1 knockout mice have a severe wasting and prolonged fasting phenotype despite increased food intake. By applying RNA sequencing and intravital microscopy, we show that loss of LKB1 leads to a dramatic reprogramming of the hepatic lobule through robust up-regulation of periportal genes and functions. This is likely mediated through the opposing effect that LKB1 has on glucagon pathways and gene expression. *Conclusion:* Our findings show that LKB1 acts as a brake to the glucagon-mediated fasting response, resulting in "periportalization" of the hepatic lobule and whole-body metabolic inefficiency. These findings reveal a mechanism by which hepatic metabolic compartmentalization is regulated by nutrient-sensing.

INTRODUCTION

Fasting is a conserved, adaptive response to nutrient deprivation that involves metabolic and transcriptional changes. The liver is critical in this response by sequentially activating catabolic and inhibiting anabolic processes to meet energy demands. Glucagon is at the crux of regulating the hepatic metabolic adaptation to fasting. When circulating glucose levels drop, glucagon stimulates hepatic glucose output through its release from glycogen storages or *de novo* synthesis through gluconeogenesis, as well as fatty acid oxidation and

Abbreviations: 2-NBDG, 2-(N-(7-nitrobenz-2-oxa-1,3-diazol-4-yl)amino)-2-deoxyglucose; AAV8, adeno-associated virus 8; AMPK, AMP-activated protein kinase; ANOVA, analysis of variance; BW, body weight; DEG, differential expression of genes; FBS, fetal bovine serum; FGF21, fibroblast growth factor 21; GLP-1, glucagon-like peptide 1; IPA, ingenuity pathway analysis; IVM, intravital microscopy; KO, knockout; LKB1, liver kinase B1; mRNA, messenger RNA; NAFLD, nonalcoholic fatty liver disease; NR4A, nuclear receptor subfamily 4 group A; PBS, phosphate-buffered saline; PC, pericentral; PCK1, phosphoenolpyruvate carboxykinase 1; PP, periportal; TBS, Tris-buffered saline; TBST, tris-buffered saline triton; WT, wild type.

Suehelay Acevedo-Acevedo and Megan L. Stefkovich contributed equally to this work.

This is an open access article under the terms of the Creative Commons Attribution-NonCommercial-NoDerivs License, which permits use and distribution in any medium, provided the original work is properly cited, the use is non-commercial and no modifications or adaptations are made.
Published 2022. This article is a U.S. Government work and is in the public domain in the USA. *Hepatology Communications* published by Wiley Periodicals LLC on behalf of American Association for the Study of Liver Diseases

ketogenesis, which provide crucial fuels to peripheral tissues during extended fasting.[1] Equally important is the ability to shut down the fasting response once nutrients become available. This action prevents catabolic processes from continuing needlessly and preventing gluconeogenesis, lipolysis, and ketogenesis to go unchecked. Indeed, impairment of fasting inhibition is observed in patients with nonalcoholic fatty liver disease (NAFLD) in whom gluconeogenesis and lipolysis are elevated.[2,3] Indeed, metformin and glucagon-like peptide 1 (GLP-1) agonists have been successful in treatment of obesity, type 2 diabetes, and NAFLD through attenuation of the glucagon response.[4–7] Fine-tuning of this complex response is temporally regulated by glucagon through activation of transcription factor cascades, leading to sequential waves of gene expression that optimize energy use and prevent tissue damage.[8]

Recently, Cheng at al. demonstrated that glucagon is also involved in the spatial regulation of hepatic metabolism.[9,10] The spatial segregation of hepatic metabolism, also known as liver zonation, permits simultaneous operation of conflicting pathways.[11–13] This is achieved through the organization of hepatocytes in polarized, hexagonal lobules in which six portal vessels deliver oxygen, nutrients, and hormones (Figure S1B) that flow directionally toward a single central vein. Several factors regulate zonation by affecting differential gene expression along the periportal (PP) to pericentral (PC) axis. For example, hypoxia and Wnt ligands activate β-catenin signaling, resulting in the expression of target genes in PC cells.[14,15] On the other hand, glucagon controls gene expression in the PP zone.[10] Although the "push and pull" relationship between Wnt ligands and glucagon have been established as a central determinant exerting zone-dependent expression patterns, it is not clear how hepatocytes integrate those signals during periods of fasting to maintain homeostasis.

One potential mediator is liver kinase B1 (LKB1), given its role as a nutrient sensor that activates AMP-activated protein kinase (AMPK) and members of the AMPK-related family. LKB1 is also an important regulator of hepatic polarity,[16–19] a feature that may be important for the spatial organization of the lobule. Loss of LKB1 in whole body[20] and liver-specific knockout[18,19,21] result in stark metabolic changes resembling cachexia, a condition that causes extreme weight loss due to fat and muscle wasting. Hepatic LKB1 was shown to be pivotal for regulating glucose homeostasis, as it is known to suppress gluconeogenesis through the activation of salt-induced kinase,[22,23] and conversely, mice lacking LKB1 display elevated hepatic gluconeogenesis,[22] driven by amino acid catabolism.[21] Furthermore, hepatic LKB1 is required for the glucose-lowering effects of metformin.[22] Despite its established involvement in whole-body homeostasis and gluconeogenesis, it is not clear how LKB1 loss of function results in such a severe metabolic phenotype.

Here, we show that hepatocyte-specific deletion of LKB1 (KO) leads to a prolonged fasting response in the liver, resulting in a severe wasting phenotype and disrupted glucose homeostasis. At the transcriptional level, liver from KO mice displayed up-regulated glucagon-induced genes throughout the hepatic lobule, many of which are enriched in PP regions in wild-type (WT) mice. Our results suggest that LKB1 fine-tunes glucagon pathways across the hepatic lobule to balance the extent of the fasting response, which is critical for whole-body energy homeostasis. These findings further our understanding of hepatic physiology and factors regulating liver zonation.

METHODS

Reagents

Primary antibodies for western blots: LKB1 (3047S, 1:1000; Cell Signaling Technologies); β-tubulin (2146S, 1:1000; Cell Signaling Technologies); phosphoenolpyruvate carboxykinase 1 (PCK1 [ab28455], 1:1000, Abcam); glyceraldehyde 3-phosphate dehydrogenase (2118S, 1:1000; Cell Signaling Technologies); Alexa Fluor 421, 647- conjugated CD324 (E-cadherin, 1:50, added during secondary antibody incubation; BioLegend); and cytochrome P450 2E1 (Cyp2e1 [ab28146], 1:200; Abcam). Secondary antibodies used: goat anti-mouse immunoglobulin G (IgG); horseradish peroxidase (HRP) conjugate (12-349, 1:1000; Millipore Sigma); goat anti-rabbit IgG, HRP conjugate (12-348, 1:1000; Millipore Sigma); Alexa-conjugated secondaries (Jackson ImmunoResearch); and Alexa Fluor 647-phalloidin (Invitrogen).

Mice

The study was approved by the National Cancer Institute (NCI)–Bethesda Animal Care and Use Committee protocol number LCMB037. C57BL/6J and LKB1 fl/fl mice (Jackson Laboratories) had free access to water and a standard diet (NIH-31 Open Formula, Envigo). Experiments were done during the light cycle.

LKB1 KO

LKB1 fl/fl were injected with adeno-associated virus 8 (AAV8; 1.25×10^{11} GC) expressing Cre recombinase under the hepatocyte thyroid hormone–binding globulin promoter (Vector Biolabs). AAV8 was delivered by tail vein injection to LKB1 fl/fl and C57BL/6J at 6 weeks of age, and mice were analyzed 4 weeks after. As expected, male mice had higher body weights and lower fat mass than female mice (data not shown).

Protein quantification

Western blot analysis was performed in whole liver homogenate from snap-frozen livers as previously described.[19] Blots were normalized to a loading control.

Liver tissue fixation, immunofluorescence staining, and histology

Whole liver was fixed using a transcardial perfusion of 4% paraformaldehyde in PBS, followed by vibratome sectioning and immunofluorescence as described previously.[19] Paraffin-embedding, sectioning, and histological staining were done by Histoserv, Inc., then scanned and evaluated by the Molecular Pathology Unit NCI.

Glucose and insulin tolerance tests

Fasted mice (6 h) were intraperitoneally injected with 0.75 units/kg insulin (Humulin R, Lilly Pharmaceuticals) or 1 g/kg 50% Dextrose (Hospira) for insulin and glucose tolerance tests, respectively. Blood was collected from the tail vein, and glucose was measured using testing strips (Ascencia Diabetes Care).

Weight and body composition analysis

To calculate the change in body weight (BW), the final BW was subtracted from the initial BW and divided by the initial BW. Body composition (fat and lean mass) was measured in unrestrained mice by Echo MRI (EchoMRI LLC, Houston, TX) at 1:00 p.m.

Food intake and energy balance analysis

Food was weighed weekly. Food intake was converted to kcal consumed/mouse/day using the energy density of the standard diet (3.1 kcal/g). Energy balance was calculated using the method described in Ravussin et al. (2013).

Serum analysis

Kits were used according to manufacturer's instructions to measure fibroblast growth factor 21 (FGF21; EZRMFGF21-26K; EMD Millipore), β-hydroxybutyrate (K632; Biovision), free fatty acid FUJIFILM (276-76491, 999-34691, 995-34791, 991-34891, 993-35191; Wako Diagnostics) and glucagon (10-1281-01; Mercodia).

Confocal microscopy and image processing

Images were acquired using a Leica SP8 inverted confocal laser scanning microscope using 63-times oil objective 1.4 Numerical aperture. E-cadherin staining was used to identify PP regions of the hepatic lobule. Images were cropped contrast-enhanced, background-subtracted, and a median filter was applied using ImageJ. Mean gray values were measured for PP and PC regions, and ratios of PC over PP were determined.

Intravital microscopy of hepatic glucose mobilization

This procedure was previously described.[24] Briefly, under anesthesia, the liver was exposed on the microscope stage (Leica SP8 inverted confocal laser). Tetramethylrhodamine-dextran (Invitrogen) was injected retro-orbitally to label the sinusoids, followed by injection of the fluorescent glucose analog during image acquisition. Quantification of glucose uptake and retention was performed as described.[24]

RNA isolation

The left lobe (three mice per group) was snap-frozen in liquid nitrogen. Approximately 20 mg per sample was homogenized (TissueLyser II; Qiagen) and RNA extracted (Qiagen #74104). RNA yield was determined using the Agilent TapeStation Instrument. Samples with a RIN > 8.0 were sent for bulk messenger RNA (mRNA) sequencing.

Bulk mRNA sequencing

The mRNA library was made with TruSeq mRNA library kit (Illumina). 200 ng of total RNA was used as the input to an mRNA capture with oligo-dT-coated magnetic beads. The mRNA was fragmented, and then a random-primed complementary DNA (cDNA) synthesis was performed. To prepare the library, the resulting double-strand cDNA was used as the input to a standard Illumina library prep with end-repair, adapter ligation, and polymerase chain reaction (PCR) amplification being performed. The final purified product was then quantitated by quantitative PCR before cluster generation and sequencing. Six mRNA-sequencing samples were pooled and sequenced on NextSeq using paired-end sequencing and a read length of 76 (2 × 76 cycles).

Sequencing data analysis

Raw data files were processed using the HiSeq Real Time Analysis software (RTA 2.11.3). Files were demultiplexed, and conversion of binary base calls and qualities into fastq format was performed using the Illumina bcl2fastq2.17. Cutadapt (version 1.18) was used to trim adapters and low-quality bases from the sequencing reads, and the trimmed reads were mapped to mouse reference genome NCBI m37/mm9 and Gencode annotation M9 using STAR (version 2.7.0f) with two-pass alignment option. RSEM (version 1.3.1) was used for gene and transcript quantification.

Raw counts files were imported into the NIH Data Analysis Portal (NIDAP) for analysis. Low counts were removed, data normalized (quantile), and batch correction was performed. Differential expression of genes (DEG) analysis was performed using Limma-Voom (bioconductor-limma package v.3.38.3), and FastGSEA (bioconductor-fgsea package v.1.8.0) was used for gene-set enrichment analysis (GSEA). Significance was determined with threshold of false discovery rate < 0.05, fold change (FC) > 1.5, FC < −1.5. Heatmaps were generated using hierarchical clustering on the NIDAP platform. The Venn diagrams were generated using Venny 2.1 (Oliveros, 2007). Data discussed in this publication have been deposited in NCBI's Gene Expression Omnibus[25] and are accessible through GEO Series accession number GSE192404 (https://www.ncbi.nlm.nih.gov/geo/query/acc.cgi?acc=GSE192404).

Statistical analysis

At least three mice were averaged per condition. Male and female values were pooled, as no sex by LKB1 KO interaction was observed. Unpaired *t*-tests were performed for data with equal variance, and a Welch's *t*-test was performed for data with unequal variance. For comparing WT and KO mice within PP or PC regions, a two-way analysis of variance (ANOVA) with Bonferroni was used, or comparing across time, a two-way repeated-measures ANOVA was used. Data are shown as mean ± SEM. Statistical significance was determined by a p-value < 0.05 (GraphPad Prism).

RESULTS

LKB1 KO mice are in a prolonged fasting state resulting in a wasting phenotype

Liver-specific LKB1 KO mice were generated via tail vein injection of AAV8 Cre recombinase with a TGB promoter in LKB1 floxed mice at 6 weeks of age and analyzed 4 weeks later. Over 90% reduction in LKB1 protein was achieved (Figure 1A) with some residual LKB1 detected, likely originating from non-parenchymal cells. As previously reported in a model in which LKB1 was depleted in neonates,[19] pAMPK levels were significantly reduced in KO livers due to loss of LKB1, which phosphorylates it (Figure S1A). Overall, KO mice were smaller than WT controls, which was also reflected by significant weight loss over the course of 4 weeks (Figure 1B,C). Weight loss occurred despite increased food intake and increase in energy expenditure, indicating poorer metabolic efficiency in KO mice (Figure 1D,E). Significant reduction in body weight from muscle and/or fat that cannot be rectified with nutritional intervention is defined as a wasting phenotype, which is also concurrent with shifts toward catabolic hepatic gene expression and metabolism.[26] Weight loss in KO mice included both fat and lean mass (Figure 1F,G). Additionally, substantial reduction in glycogen storage was observed in liver sections from KO mice, primarily around PC and midlobular regions (Figure 1H,I and Figure S2). Hematoxylin and eosin and terminal deoxynucleotidyl transferase–mediated deoxyuridine triphosphate nick-end labeling staining did not reveal signs of inflammation or tissue damage (Figure S2). The wasting phenotype observed is consistent with previous reports in whole body[20] and liver-specific LKB1 KO models.[18,19,21] Previously, we have shown that deletion of LKB1 at birth via albumin Cre excision displayed a similar phenotype to the one we describe here using AAV8 Cre injection in mature mice.[19] Together, this demonstrates a vital role for hepatic LKB1 in maintaining metabolic homeostasis in both neonate and adult mice.

Because LKB1 was ablated specifically in hepatocytes, we next examined whether KO livers will be a source for elevated markers of prolonged fasting/starvation. Ketone bodies are produced in the liver during extended fasting, starvation, or exercise (Rui [2014]; White and Venkatesh [2011]) through fatty acid oxidation (Puchalska and Crawford [2017]). Indeed, serum level of the ketone body β-hydroxybutyrate was increased in KO mice (Figure 1J). In addition, we measured serum levels of starvation-associated hormone FGF21[27] and found it was higher in KO mice (Figure 1K). FGF21 levels have been shown to promote lipolysis in diet-induced obese mice, leading to weight loss.[28] Additionally, FGF21 null mice are protected from muscle loss,[29] and elevated FGF21 is associated with sarcopenia in adults.[30] This catabolic role of FGF21 on muscle mass likely explains the reduction in muscle observed in KO mice. Consistently, serum free fatty acid levels were also elevated in KO mice (Figure 1L). Despite these elevated markers of prolonged fasting, serum glucagon levels in KO mice were significantly reduced (Figure 1M), likely driven

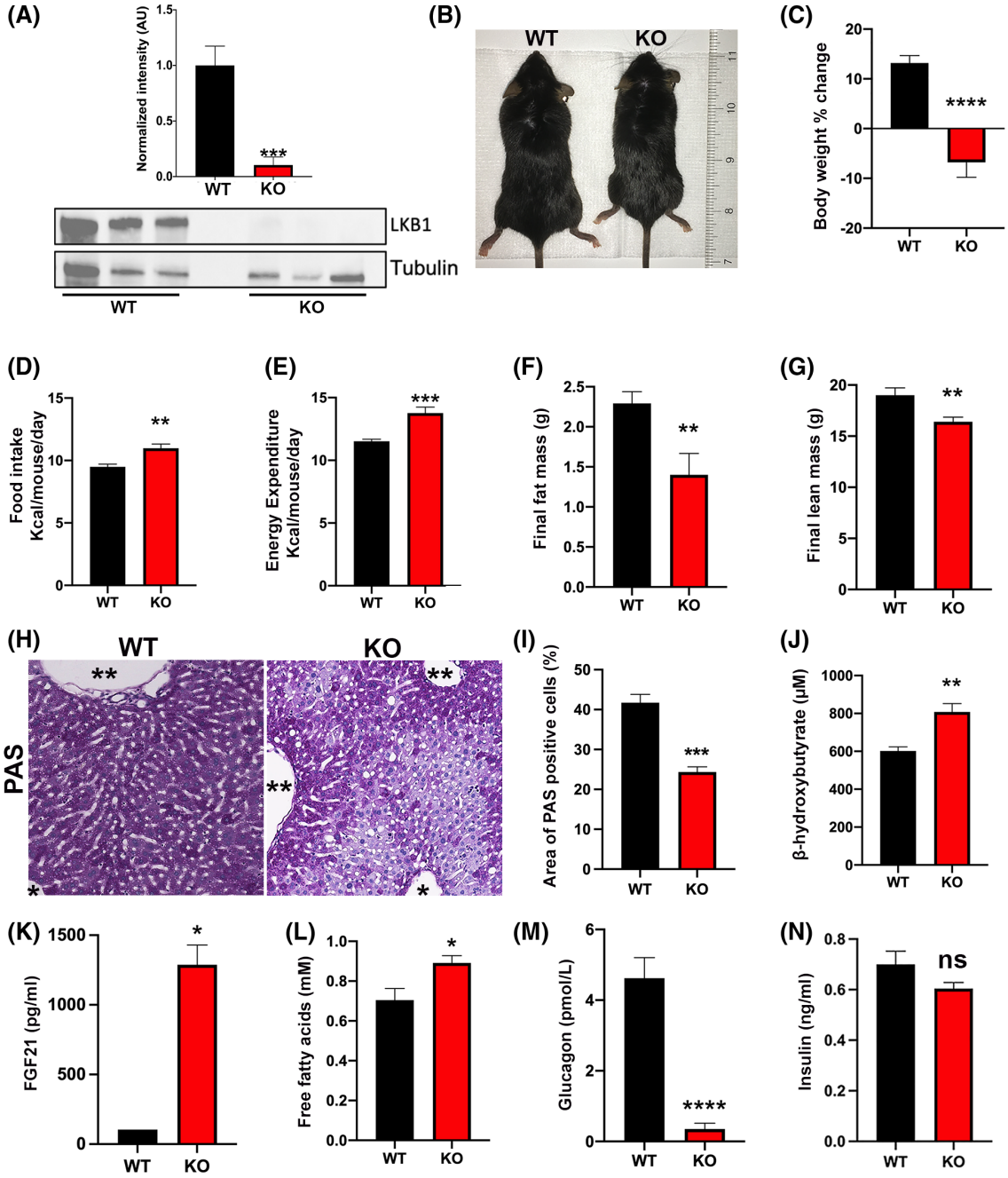

FIGURE 1 Characterization of changes in whole-body energy homeostasis in wild-type (WT) and knockout (KO) mice. (A) Confirmation of liver kinase B1 (LKB1) ablation in the liver. (B) Representative image of WT and KO mice. (C) Percent change in body weight. (D) Daily food intake (average values from 4-week-long measurements). (E) Energy expenditure measured per mouse per day (average values from 4-week-long measurements). (F) Final fat mass. (G) Final lean mass. (H) Analysis of liver glycogen using periodic acid–Schiff (PAS) staining in liver sections from WT and KO. **Portal vessel; *central vein. (I) Quantification of PAS-positive hepatocytes expressed by percentage of area. (J) Serum levels of b-hydroxybutyrate. (K) Serum levels of fibroblast growth factor 21 (FGF21). (L) Serum levels of free fatty acids. (M,N) Serum glucagon (M) and serum insulin (N) in WT and KO mice. In all of these experiments, n = 16–18 mice per measurement. Data are shown as mean ± SEM. p-Values were calculated using an unpaired Student's t-test. *$p < 0.05$, **$p < 0.005$, ***$p < 0.0005$, ****$p < 0.0001$. ns, not significant

by the hyperglycemia in KOs (Figure 2A), and as previously reported.[22,23] On the other hand, insulin levels were unchanged (Figure 1N). Collectively, these results demonstrate that the liver is in a prolonged fasting state, consistent with the observed wasting phenotype.

Glucose retention is reduced in LKB1 KO hepatocytes

LKB1 ablation results in sever disruption to glucose homeostasis.[22,23] Consistently, KO mice were hyperglycemic (Figure 2A) and displayed glucose intolerance

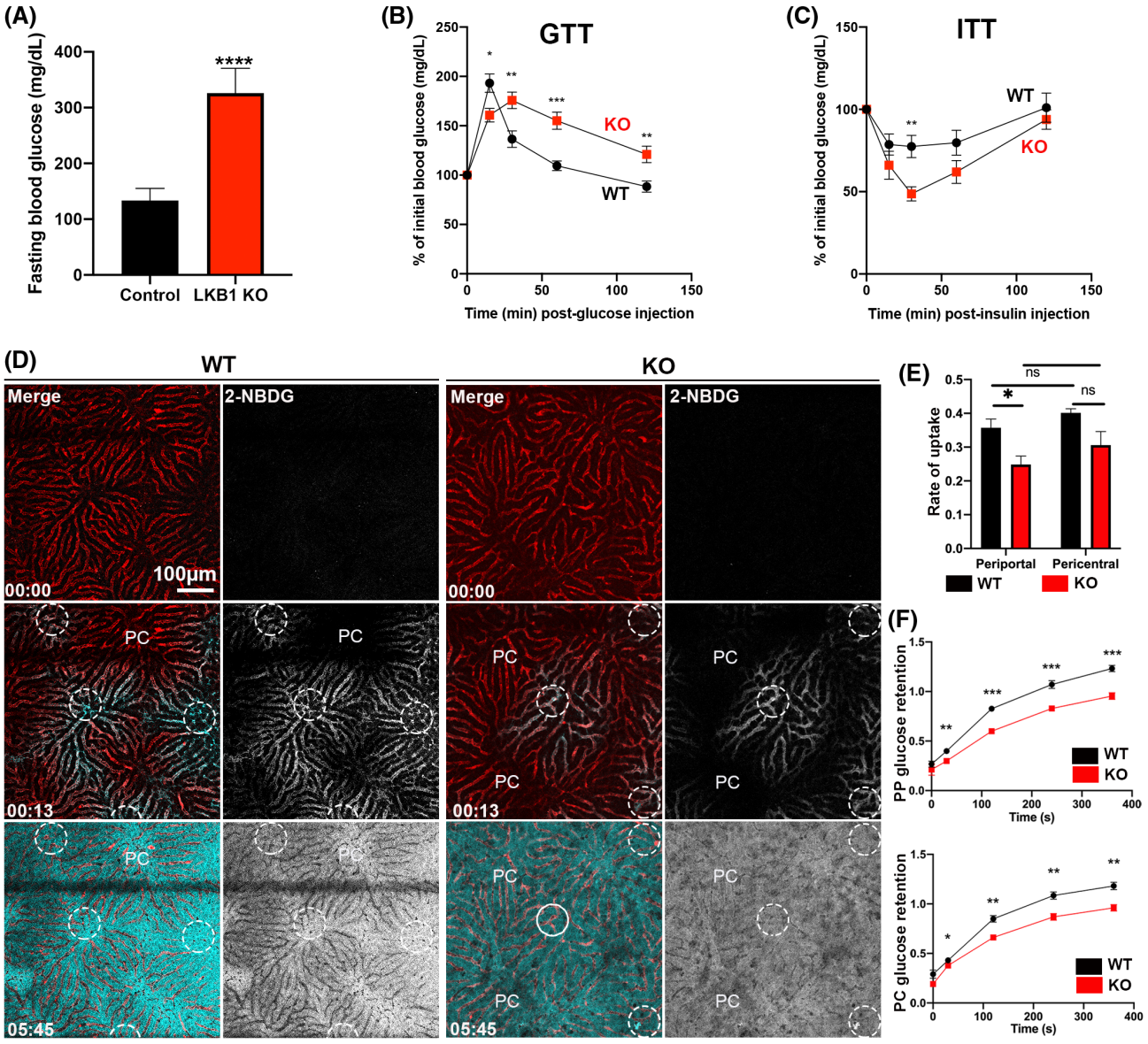

FIGURE 2 Intravital microscopy (IVM) of glucose uptake and retention in WT and KO mice. (A) Fasting blood glucose from WT and KO mice. (B,C) Glucose tolerance test (GTT) (B) and insulin tolerance test (ITT) (C) of WT and KO mice. (D) Representative time-lapse frames of hepatic glucose uptake *in vivo* using the fluorescent glucose probe 2-(N-[7-nitrobenz-2-oxa-1,3-diazol-4-yl]amino)-2-deoxyglucose (2-NBDG; white). Mice were injected with 2-NBDG approximately 10 s into image acquisition. Dextran (red) was used to label the vasculature (time = min: s). Dashed white circles indicate portal veins. (E) Quantification of glucose uptake rate (positive pixels/second). (F) Quantification of glucose retention shown as the ratio of mean fluorescence intensity of 2-NBDG in hepatocytes to sinusoids in periportal (PP) hepatocytes and pericentral (PC) hepatocytes. Scale bar = 100 μm. Data are shown as mean ± SEM. *p*-Values were calculated using an unpaired Student's *t*-test for fasting glucose, a two-way analysis of variance (ANOVA) for WT versus KO within PP or PC, or repeated-measures two-way ANOVA for WT versus KO across time ($n = 3$ mice). *$p < 0.05$, **$p < 0.005$, ***$p < 0.0005$, and ****$p < 0.00001$. CV, central vein; ns, not significant

(Figure 2A,B), but were insulin-sensitive (Figure 2C), indicating peripheral tissues were responding appropriately. Glucose homeostasis is maintained by the coordination of glucose synthesis, storage and use, which vastly differ across the hepatic lobule.[12] This led us to examine whether glucose uptake and release is spatially regulated, and whether LKB1 has a role in it. To this aim, we developed an assay to measure hepatic glucose mobilization in live anesthetized mice using time-lapse intravital microscopy (IVM)[24] using fluorescent glucose analog 2-NBDG (2-[N-(7-nitrobenz-2-oxa-1,3-diazol-4-yl)amino]-2-deoxyglucose; Figure 2D–F). With this approach, the rate of glucose uptake and retention in PP and PC hepatocytes was measured. In WT mice, 2-NBDG signal appeared in portal vein areas within seconds of injection and was taken up by hepatocytes over the course of 6 min (Figure 2D, Movie S1). Although serum glucose concentrations are reportedly higher in the portal vein,[31] we found no difference in the rate

of glucose uptake between PP and PC hepatocytes in WT mice (Figure 2E). However, in KO mice, the rate of uptake in both PP and PC hepatocytes was significantly lower compared with WT, and accumulation of 2-NBDG signal was not observed in PC regions (Figure 2E). Additionally, we compared the ability of the hepatocytes to retain glucose by calculating the ratio of 2-NBDG fluorescent signal in hepatocytes over sinusoids. Hepatic glucose retention was significantly decreased in KO mice in PP and PC regions, suggesting that glucose is released rather than stored (Figure 2F) and consistent with the hyperglycemia and reduced glycogen. This study evaluates glucose mobilization in a spatially resolved manner and provides insights into glycemic control.

Up-regulation of PP-enriched genes and pathways in LKB1 KO mice

To identify the drivers of these metabolic changes in LKB1-deficient livers, we performed RNA sequencing and examined its impact on gene expression. Out of 11,669 identified genes, 1635 were differentially expressed in the KO liver compared with WT, with an approximate 1:1 ratio of up-regulated to down-regulated genes (Figure 3A and Table S1). GSEA and Ingenuity Pathway Analysis (IPA) were used to analyze the DEGs. We found 699 significantly enriched pathways, a subset of which is shown in Figure 3B. Interestingly, many pathways that are associated with PP-related functions including mitochondria oxidative phosphorylation (Figure S3A,B), trichloroacetic acid cycle, the previously reported gluconeogenesis,[23] and amino acid catabolism,[21] were enriched in KO hepatocytes (Figure 3B). These pathways are up-regulated in the fasted liver,[32] supporting the observation that LKB1 KO livers are in a fasting state. Pathways associated with PC-related functions, on the other hand, such as lipogenesis and bile acid metabolism, were down-regulated (Figure 3B), suggesting a bias toward PP-enriched genes in the KO liver. To investigate this idea further, we used a list of PP-enriched and PC-enriched genes compiled by Cheng et al.[10] and compared them with the DEGs identified in the LKB1 KO mice. Indeed, out of 270 PP and 461 PC genes, 89 and 157 were regulated in the LKB1 KO livers, respectively. Strikingly, within these regulated genes, there was substantial up-regulation of PP-enriched and down-regulation of PC-enriched genes (Figure 3C,D), suggesting the involvement of LKB1 in the spatial division of metabolic functions.

Given these changes in zone-restricted gene expression in KO livers, immunofluorescence localization studies were performed to examine the spatial distribution of selected enzymes in liver sections. Based on gene expression, gluconeogenesis is enriched to PP hepatocytes.[12] Consistently, protein expression of the rate-limiting enzyme PCK1 was mostly confined to PP hepatocytes in WT (Figure 3E upper image). However, in the KO lobule, PCK1 expression increased, and its distribution became uniform across both PP and PC hepatocytes (Figure 3E lower image). Fluorescence intensity ratios (PC/PP) demonstrate the increase in PCK1 expression levels in PC regions (Figure 3F), while the line scan demonstrates the loss of PCK1 zonation in KO mice (Figure 3G, solid red line). Overall, in the WT mice, PCK1 expression is barely detected in PC regions, whereas in the KO mice it is present across the lobule, suggesting a loss of functional zonation (Figure 1G). Similar results were obtained with the PP urea cycle enzyme arginase 1 (Figure S3C–E). The spatial localization of PC enzymes was also investigated, including Cyp2e1, which is involved in xenobiotic metabolism. Cyp2e1 is mostly confined to PC hepatocytes in the WT, and this pattern was lost in KO due to reduced expression levels of the enzyme and restricted distribution around the central vein (Figure 3H–J). Similar results were obtained with the PC lipogenic enzyme acetyl-CoA carboxylase 1 (Figure S3F–H). Overall, in the absence of LKB1, the liver defaults to a PP metabolic program that overrides PC-related gene expression and functions. This loss in zonation and uniform distribution of PP enzymes indicates that LKB1 signaling is important in maintaining liver zonation.

LKB1 regulates glucagon target genes, but not Wnt/b-catenin

To understand how LKB1 affects liver zonation IPA analysis was performed to identify potential regulators based on the DEG. Interestingly, glucagon was identified as the top upstream activator of LKB1 (Figure 4A). Because glucagon was reported to regulate liver zonation by promoting the expression of PP genes,[10] we next investigated the relationship between LKB1-regulated and glucagon-regulated genes. To this aim, DEG identified in LKB1 KO was compared with those identified in glucagon KO mice.[10] Glucagon KO mice were selected for this comparison because, like the LKB1 KO, they displayed low serum glucagon. Of the 297 DEGs identified in glucagon KO livers, 40% overlapped with DEGs in LKB1 KO (Figure 4B and Table S2). Interestingly, the overlapping genes inversely correlated (Figure 4C), suggesting that LKB1 has an overall inhibitory effect on glucagon-related gene expression. In glucagon KO mice, PC genes were up-regulated.[10] In LKB1 KO mice, despite reduced glucagon levels (Figure 1M), PP-enriched genes were enhanced, thus reinforcing the notion that LKB1 negatively regulates glucagon-related transcriptional changes. Similar analysis of Wnt target genes revealed that of the 1003 DEGs, 20% of the LKB1 KO overlapped (Figure 4D and

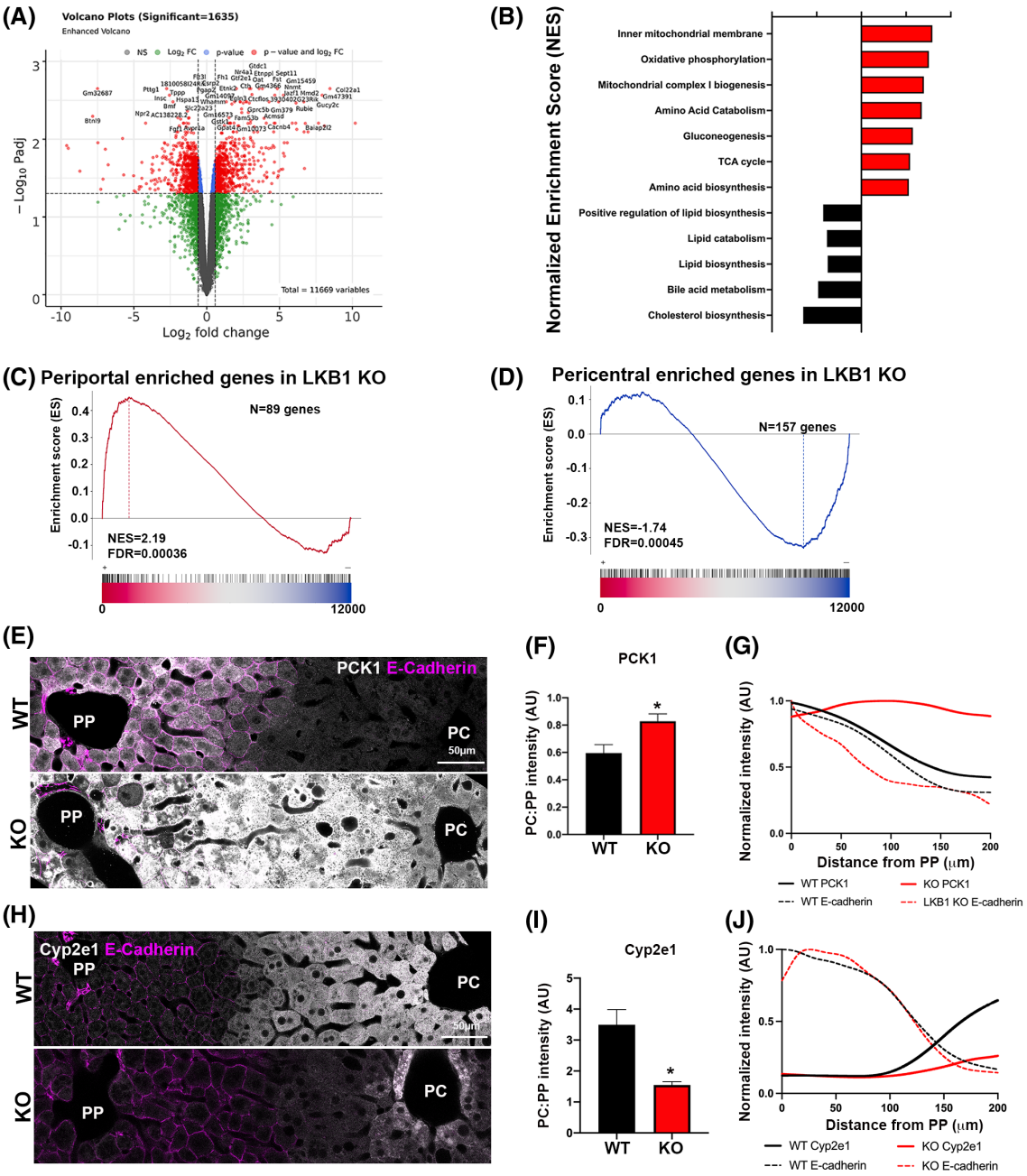

FIGURE 3 LKB1 regulates PP genes and function. (A) Volcano plot showing global gene expression from WT and KO livers (n = 3 mice per group). (B) Enrichment of select up-regulated (red) and down-regulated (black) pathways in KO mice. (C,D) Gene-set enrichment plots showing expression of PP-associated (C) and PC-associated genes (D), upper and lower graphs, respectively, in LKB1 KO livers. Gene list from Cheng et al.[10] was used for the comparison. (E) Immunofluorescence showing phosphoenolpyruvate carboxykinase 1 (PCK1; gray) localization in WT and KO liver sections. PP regions are labeled with E-cadherin (magenta). (F) Quantification of PCK1 expression is shown as the ratio of PCK1 mean gray value in PC and PP hepatocytes. (G) Line scan of fluorescence intensity across the lobule showing PCK1 distribution. Note that PP-enriched distribution in WT mice is lost in the absence of LKB1 and becomes uniform. (H) Immunofluorescence showing Cyp2e1 (gray) localization in WT and KO liver sections. PP regions are labeled with E-cadherin (magenta). (I) Quantification of Cyp2e1 expression is shown as the ratio of Cyp2e1 mean gray value in PC and PP. (J) Line scan of fluorescence intensity across the lobule showing Cyp2e1 distribution. Note that PC-enriched distribution in WT mice is barely detected in the absence of LKB1. Four 8 PP or PC regions were analyzed per mouse and averaged (n = 3 mice per group). Scale bar = 50 μm. Data are shown as mean ± SEM; p-values were calculated using an unpaired Student's t-test or a Welch's t-test. FDR, false discovery rate; NES, normalized enrichment score; TCA, trichloroacetic acid cycle

Table S3). However, there was no correlation in expression between the overlapping genes (Figure 4E). These results suggest that up-regulation in PP-enriched and decreased PC-enriched gene expression in LKB1 deficient hepatocytes is driven by uninhibited glucagon-related pathways rather than changes to Wnt/b-catenin.

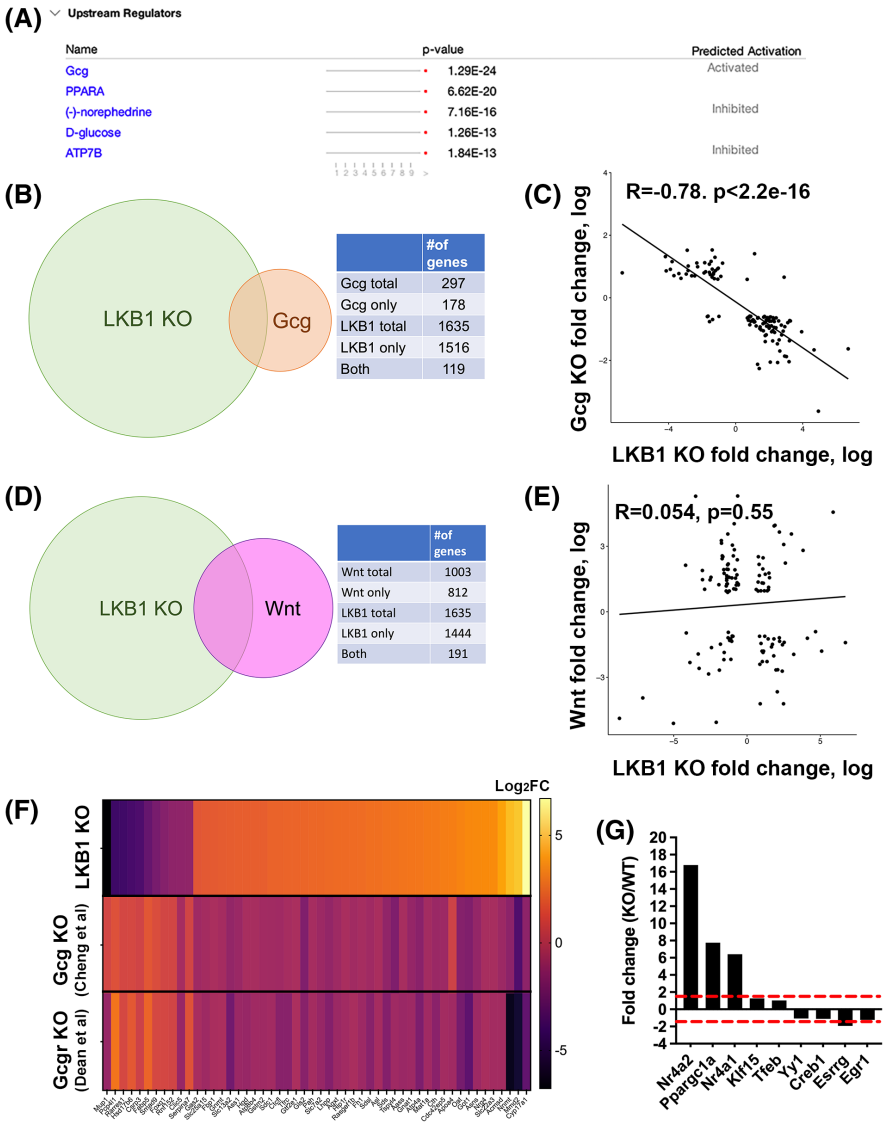

FIGURE 4 LKB1 negatively regulates glucagon-induced genes, but not Wnt-regulated genes. (A) Upstream regulators of LKB1 identified using Ingenuity Pathway Analysis (IPA). (B) Venn diagram of differentially expressed genes in LKB1 KO (current study) and glucagon KO[10] showing 119 overlapping genes. (C) The correlation between LKB1 KO and glucagon KO genes. (D) Venn diagram of differentially expressed genes in LKB1 KO (current study) and Wnt-regulated,[42,50] showing 191 overlapping genes. (E) The correlation between LKB1 KO and Wnt-regulated genes. (F) Heat map of representative differentially expressed genes in LKB1 KO, glucagon (Gcg) KO[10] and Gcg receptor (Gcgr) KO.[33] (G) Fold change of transcription factors in WT versus LKB1 KO mice. Abbreviations: ATP7B, atpase copper transporting beta; Creb1, cAMP responsive element binding protein 1; Egr1, early growth response 1; Esrrg, estrogen related receptor gamma; Klf15, kruppel like Factor 15; NR4A1/2, nuclear receptor subfamily 4 group A member 1/2; PPARA, peroxisome proliferator activated receptor alpha; Tfeb, transcription factor EB; Yy1, ying yang 1

To confirm this, we also compared DEGs from LKB1 KO with those reported in liver-specific glucagon receptor KO mice.[33] Of the 1744 DEGs identified in glucagon receptor KO livers, 15% overlapped with DEGs in LKB1 KO (Figure S4 and Table S4), and their expression displayed a significant inverse correlation again (Figure S4A,B). A heatmap of the common affected genes in LKB1 KO, glucagon KO, and glucagon receptor KO are shown in Figure 4F and Table S5. We posit that LKB1 acts as a brake for glucagon-related gene expression. Once that brake is gone (i.e., LKB1 KO), the negative feedback loop is broken, allowing glucagon-related pathways to increase unregulated. This notion is reinforced by the fact that glucagon-related genes are elevated in the face of low serum glucagon levels in LKB1 KO mice.

Glucagon is involved in the hepatic fasting response through activation of transcription factors. Initially, glucagon stimulates the cyclic adenosine monophosphate/CREB pathway, which leads to expression of additional transcription factors and a second wave of gene expression facilitating the temporal regulation of the fasting response.[8] Therefore, expression levels of transcription factors involved in the hepatic fasting response in the

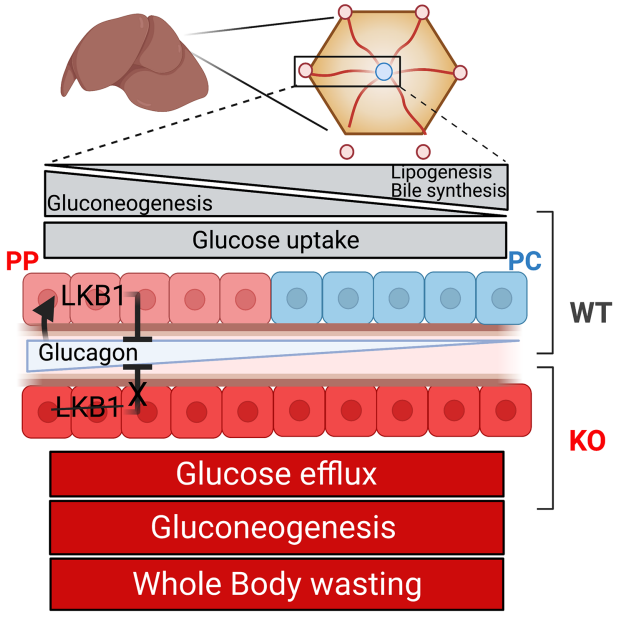

FIGURE 5 Graphical summary of results, showing how loss of LKB1 allows glucagon genes to be up regulated, leading to metabolic inefficiency and periportalization of the lobule

LKB1 KO were examined. Significant increases in nuclear receptor subfamily 4 group A member 1 (Nr4a1; 6-fold) and member 2 (Nr4a2; 16-fold) were found in KO mice (Figure 4G). These factors are involved in up-regulating gluconeogenesis and the expression of FGF21.[34,35] Additionally, increased expression of Ppargc1a (7-fold) was observed, which was previously described in LKB1 KO mice,[22] and is involved in FAO and ketogenesis.[36] These transcription factors are part of the delayed response to glucagon and may explain the exacerbated and prolonged hepatic fasting phenotype (Figure 1). Finally, Figure 5 summarizes our findings in a model. We propose a negative feedback loop in which LKB1 keeps the glucagon-related hepatic fasting response under control. Depletion of LKB1 results in unrestrained activation of glucagon-related pathways including gluconeogenesis, glucose efflux, ketogenesis, and lipolysis. These zone-restricted functions extend across the hepatic lobule in mutant mice, leading to loss of liver zonation. These findings explain the wasting phenotypes resulting in overall weight loss, inability to store fuels, and metabolic inefficiency. Additionally, this study highlights the possibility that glucagon-related hepatic fasting is not only transcriptionally controlled in time,[8] but also spatially regulated by LKB1 across the hepatic lobule.

DISCUSSION

Fasting is an essential adaptive response to simultaneously mobilize nutrients as a fuel source while conserving energy expenditure. During diseases such as NAFLD and type 2 diabetes, an inability to shut down this fasting response results in persistent gluconeogenesis and lipolysis,[37] despite adequate nutrient consumption. This excessive mobilization of fuels worsens the inability to arrest the fasting response, and further exacerbates disease progression. Here, we show that LKB1 is vital for the inhibition of the hepatic fasting response. Our findings that LKB1 KO mice have a wasting phenotype (Figure 1) despite increased food intake (Figure 1D), and circulating substrates in the blood (Figures 1J–N and 2A) are indicative of disruption in the homeostatic control of energy balance and suggestive of overall metabolic inefficiency. Energy expenditure allows the evaluation of overall metabolic efficiency by measuring the ability to convert ingested energy into fat and protein.[38] In an attempt to maintain bodyweight during fasting, energy expenditure is decreased by reducing physical activity[39] and diet-induced thermogenesis.[40] Supporting this, Just et al. previously showed that liver-specific LKB1 KO had decreased locomotor activity.[21] However, we measured significantly higher energy expenditure in KO mice despite being in a phenotypical hepatic fasting state (Figure 1E), reflecting metabolic inefficiency in LKB1 KO mice. Although we do not know the cause for this inefficiency, the dramatic reduction in hepatocyte heterogeneity reported here may lead to impaired division of liver function, causing reduced efficiency. Alternatively, it is possible that due to the severe hyperglycemia in KO mice, the diet-induced thermogenesis is increased.

One of the key phenotypes described in LKB1 KO mice is dysregulated glucose homeostasis.[21–23] Hepatocytes shift between glucose uptake for storage in the fed state and release during the fasted states. Despite the fact that glucose uptake, storage, and efflux are differentially regulated across the hepatic lobule,[12,13] it is not clear whether LKB1 is involved and how. To measure the changes in glucose uptake and release, we developed an IVM-based assay to measure glucose mobilization in space and time.[24] We measured markedly reduced glucose uptake and retention in KO hepatocytes, indicating that they are in constitutive efflux state (Figure 2D–F). These results are consistent with the severe hyperglycemia and glucose intolerance (Figure 2A,B), reduced glycogen storage (Figure 1H,I), and up-regulation of gluconeogenesis genes (Figure 3B–E). Interestingly, Berndt et al. used modeling to propose that PP hepatocytes release and PC hepatocytes take up glucose.[41] However, *in vivo*, we did not detect any difference in the rate of glucose uptake and/or retention between PP and PC hepatocytes in WT or KO (Figure 2D,E). Similar kinetics in PP and PC are likely achieved through differential expression of high-affinity and low-affinity glucose transporters across the lobule [12] and redistribution of these transporters when glucose availability shifts. This study

shows that LKB1 plays a vital role in the spatial metabolism of glucose in the liver. Our results underscore the importance of measurements of physiological parameters in the intact tissue.

This unique spatial organization of hepatocytes (Figure 5 and Figure S1E) results in the formation of nutrient, oxygen, hormone, and morphogen gradients, which in turn shape hepatocytes' gene expression. Indeed, a recent study using single-cell RNA sequencing demonstrated that 50% of liver genes are zonated.[42] Key regulators of this zonation were identified and include Wnt/b-catenin, glucagon, hypoxia, H-ras, and growth and thyroid hormones.[12] However, these do not account for all the zonated genes, highlighting the existence of additional regulators of zonation. Our findings show that LKB1 plays a significant role in liver zonation. In the absence of LKB1, the spatial division of hepatic metabolism is abolished. Instead, we observed a striking up-regulation of PP-associated genes, expansion of their spatial distribution, and down-regulation of PC-related genes (Figure 3B–D and Figure S3A,B). In a previous study, Cheng et al. showed that glucagon oppose Wnt/b -catenin activity by inducing PP gene expression.[10] Our analysis identified glucagon as a probable upstream activator of LKB1. Furthermore, we show a strong inverse correlation between glucagon and LKB1 regulated genes. This apparent interplay between glucagon and LKB1 indicates a possible fine-tuning of the hepatocyte's response to glucagon, although additional studies are warranted to confirm this. We propose a negative feedback loop between glucagon and LKB1, leading to fine-tuning of hepatocyte's response to glucagon. Indeed, Cheng et al. showed that glucagon ablation led to down-regulation of PP-associated pathways and up-regulation of PC ones, reinforcing the notion that LKB1 influences glucagon signaling.[43] This type of regulation is reminiscent of the balancing act between Wnt/b-catenin and its negative regulator adenomatous polyposis coli protein in the regulation of PC genes.[44,45] Previous reports also indicated a cross talk between LKB1 and Wnt signaling in different models.[46–48] However, our data show no correlation between the expression of Wnt targets and LKB1-regulated genes (Figure 4D,E), suggesting that the effects of LKB1 on zonation are largely independent of Wnt. Although mechanistic studies to elucidate how LKB1 counterbalances glucagon are warranted, we propose that hepatocyte nutrient sensing through LKB1, together with extrinsic factors such as glucagon, orchestrate the patterned gene expression observed in the hepatic lobule. This study is focused on glucagon; however, we did not rule out that other factors such as corticosterone and epinephrin could contribute to the phenotype.

Our study demonstrates that loss of LKB1 in the liver leads to a prolonged hepatic fasting response, which contributes to weight loss, decreased glycogen, lean and adipose mass, and an overall decrease in metabolic efficiency (Figure 1). We identify LKB1 as a vital inhibitor of the glucagon-related hepatic fasting response, to prevent a wasting phenotype. We posit that LKB1 acts as an important brake in the negative feedback loop of glucagon signaling in the liver. One possibility is that LKB1 interacts with transcription factors in the nucleus and affects their activity. It was previously shown that the transcription factor Nr4a1 (Nur77) binds and sequesters LKB1 in the nucleus, thereby attenuating AMPK activation.[49] In turn, this interaction may also regulate the activity of transcription factors and, like shown in this study, lead to an overall up-regulation of glucagon-related genes. Attenuation of the glucagon response via metformin and GLP-1 agonists has become one of the most effective drug targets for obesity, type 2 diabetes, and NAFLD.[4,6] Therefore, increasing our understanding of the regulatory mechanisms behind glucagon signaling is vital to improve new pharmacological therapeutics. Here, the wasting phenotype caused by uncontrolled glucagon-related gene expression in the liver was observed alongside complete ablation of metabolic zonation in the hepatic lobule, raising the provocative possibility that the fasting response is not only regulated transcriptionally in time,[8] but also in space within the hepatic lobule. This could be critical for the organism's survival in sustaining the fasting response if nutrients are unavailable. The lobule's anatomy allows for increased capacity of PP-like hepatocytes, and glucagon-LKB1 signaling axis may be at the nexus of the spatio-temporal regulation of the fasting response. While confirming previous reports of body weight loss[19–21] and reduced muscle mass[21] in LKB1 KO mice, this paper extends these findings to demonstrate a role for LKB1 in modulating the hepatic fasting response through glucagon-induced genes and overall impact on liver zonation, Furthermore, we show the disruption in glucose homeostasis in LKB1 KO mice with spatial and temporal resolution. Given the conserved role of LKB1 in cell polarity, it is possible that it is also involved in the organization of the hepatic lobule, which represents polarity in the tissue scale. Mechanistically, it is unclear how these zone-specific changes influence metabolic efficiency seen in LKB1 KO mice. Future studies that attempt to restore liver zonation and rescue the wasting phenotype in LKB1 KO mice would identify its disruption as the primary cause of metabolic inefficiency in these mice. Nonetheless, this study reveals a mechanism by which hepatic metabolic compartmentalization is regulated by nutrient sensing.

ACKNOWLEDGMENT

The authors thank members of the Porat-Shliom lab; Drs. Will Printz, Win Arias, and Julie Donaldson for critical reading of the manuscript; Dr. Oksana Gavrilova from the NIDDK Mouse Metabolism Core for mouse phenotyping studies; CCR Sequencing Facility at the

Frederick National Laboratory for Cancer Research; and Dr. Alexei Lobanov from the CCR Collaborative Bioinformatics Resource.

CONFLICT OF INTEREST

Nothing to report.

ORCID

Natalie Porat-Shliom https://orcid.org/0000-0003-2676-8483

REFERENCES

1. Jiang G, Zhang BB. Glucagon and regulation of glucose metabolism. Am J Physiol Endocrinol Metab. 2003;284:E671–8.
2. Samuel VT, Shulman GI. Nonalcoholic fatty liver disease as a nexus of metabolic and hepatic diseases. Cell Metab. 2018;27:22–41.
3. Seppala-Lindroos A, Vehkavaara S, Hakkinen AM, Goto T, Westerbacka J, Sovijarvi A, et al. Fat accumulation in the liver is associated with defects in insulin suppression of glucose production and serum free fatty acids independent of obesity in normal men. J Clin Endocr Metab. 2002;87:3023–8.
4. Rosenstock J, Wysham C, Frías JP, Kaneko S, Lee CJ. Efficacy and safety of a novel dual GIP and GLP-1 receptor agonist tirzepatide in patients with type 2 diabetes (SURPASS-1): a double-blind, randomised, phase 3 trial. Lancet. 2021;398:143–55. https://doi.org/10.1016/s0140-6736(21)01324-6
5. Drucker DJ. Mechanisms of action and therapeutic application of glucagon-like peptide-1. Cell Metab. 2018;27:740–56.
6. Wilding JPH, Batterham RL, Calanna S, Davies M, Van Gaal LF, Lingvay I, et al. Once-weekly semaglutide in adults with overweight or obesity. N Engl J Med. 2021;384:989–1002.
7. Miller RA, Chu QW, Xie JX, Foretz M, Viollet B, Birnbaum MJ. Biguanides suppress hepatic glucagon signalling by decreasing production of cyclic AMP. Nature. 2013;494:256–60.
8. Goldstein I, Hager GL. The three Ds of transcription activation by glucagon: direct, delayed, and dynamic. Endocrinology. 2018;159:206–16.
9. Ravnskjaer K, Madiraju A, Montminy M. Role of the cAMP pathway in glucose and lipid metabolism. Handb Exp Pharmacol. 2016;233:29–49.
10. Cheng X, Kim SY, Okamoto H, Xin Y, Yancopoulos GD, Murphy AJ, et al. Glucagon contributes to liver zonation. Proc Natl Acad Sci USA. 2018;115:E4111–9.
11. Jungermann K, Sasse D. Heterogeneity of liver parenchymal cells. Trends Biochem Sci. 1978;3:198–202. https://doi.org/10.1016/s0968-0004(78)91764-4
12. Ben-Moshe S, Itzkovitz S. Spatial heterogeneity in the mammalian liver. Nat Rev Gastroenterol Hepatol. 2019;16:395–410.
13. Cunningham RP, Porat-Shliom N. Liver zonation—revisiting old questions with new technologies. Front Physiol. 2021;12:732929.
14. Kietzmann T. Metabolic zonation of the liver: the oxygen gradient revisited. Redox Biol. 2017;11:622–30.
15. Preziosi M, Okabe H, Poddar M, Singh S, Monga SP. Endothelial Wnts regulate beta-catenin signaling in murine liver zonation and regeneration: a sequel to the Wnt-Wnt situation. Hepatol Commun. 2018;2:845–60.
16. Fu D, Wakabayashi Y, Ido Y, Lippincott-Schwartz J, Arias IM. Regulation of bile canalicular network formation and maintenance by AMP-activated protein kinase and LKB1. J Cell Sci. 2010;123:3294–302.
17. Fu D, Wakabayashi Y, Lippincott-Schwartz J, Arias IM. Bile acid stimulates hepatocyte polarization through a cAMP-Epac-MEK-LKB1-AMPK pathway. Proc Natl Acad Sci USA. 2011;108:1403–8.
18. Homolya L, Fu D, Sengupta P, Jarnik M, Gillet JP, Vitale-Cross L, et al. LKB1/AMPK and PKA control ABCB11 trafficking and polarization in hepatocytes. PLoS One. 2014;9:e91921.
19. Porat-Shliom N, Tietgens AJ, Van Itallie CM, Vitale-Cross L, Jarnik M, Harding OJ, et al. Liver kinase B1 regulates hepatocellular tight junction distribution and function in vivo. Hepatology. 2016;64:1317–29.
20. Shan T, Xiong Y, Kuang S. Deletion of Lkb1 in adult mice results in body weight reduction and lethality. Sci Rep. 2016;6:36561.
21. Just PA, Charawi S, Denis RGP, Savall M, Traore M, Foretz M, et al. Lkb1 suppresses amino acid-driven gluconeogenesis in the liver. Nat Commun. 2020;11:6127.
22. Shaw RJ, Lamia KA, Vasquez D, Koo SH, Bardeesy N, Depinho RA, et al. The kinase LKB1 mediates glucose homeostasis in liver and therapeutic effects of metformin. Science. 2005;310:1642–6.
23. Patel K, Foretz M, Marion A, Campbell DG, Gourlay R, Boudaba N, et al. The LKB1-salt-inducible kinase pathway functions as a key gluconeogenic suppressor in the liver. Nat Commun. 2014;5:4535.
24. Stefkovich ML, Kang SWS, Porat-Shliom N. Intravital microscopy for the study of hepatic glucose uptake. Curr Protoc. 2021;1:e139.
25. Edgar R, Domrachev M, Lash AE. Gene expression omnibus: NCBI gene expression and hybridization array data repository. Nucleic Acids Res. 2002;30:207–10.
26. Kays JK, Shahda S, Stanley M, Bell TM, O'Neill BH, Kohli MD, et al. Three cachexia phenotypes and the impact of fat-only loss on survival in FOLFIRINOX therapy for pancreatic cancer. J Cachexia Sarcopenia Muscle. 2018;9:673–84.
27. Lin XL, Liu YB, Hu HJ. Metabolic role of fibroblast growth factor 21 in liver, adipose and nervous system tissues. Biomed Rep. 2017;6:495–502.
28. Inagaki T, Dutchak P, Zhao G, Ding X, Gautron L, Parameswara V, et al. Endocrine regulation of the fasting response by PPARalpha-mediated induction of fibroblast growth factor 21. Cell Metab. 2007;5:415–25.
29. Oost LJ, Kustermann M, Armani A, Blaauw B, Romanello V. Fibroblast growth factor 21 controls mitophagy and muscle mass. J Cachexia Sarcopeni. 2019;10:630–42.
30. Jung HW, Park JH, Kim D, Jang IY, Park SJ, Lee JY, et al. Association between serum FGF21 level and sarcopenia in older adults. Bone. 2021;145:115877.
31. Pagliassotti MJ, Myers SR, Moore MC, Neal DW, Cherrington AD. Magnitude of negative arterial-portal glucose gradient alters net hepatic glucose balance in conscious dogs. Diabetes. 1991;40:1659–68.
32. Sokolović M, Sokolović A, Wehkamp D, van Themaat EVL, de Waart DR, Gilhuijs-Pederson LA, et al. The transcriptomic signature of fasting murine liver. BMC Genom. 2008;9. https://doi.org/10.1186/1471-2164-9-528
33. Dean ED, Li M, Prasad N, Wisniewski SN, Von Deylen A, Spaeth J, et al. Interrupted glucagon signaling reveals hepatic α cell axis and role for L-glutamine in α cell proliferation. Cell Metabolism. 2017;25:1362–73.e5. https://doi.org/10.1016/j.cmet.2017.05.011
34. Pei L, Waki H, Vaitheesvaran B, Wilpitz DC, Kurland IJ, Tontonoz P. NR4A orphan nuclear receptors are transcriptional regulators of hepatic glucose metabolism. Nat Med. 2006;12:1048–55.
35. Min AK, Bae KH, Jung YA, Choi YK, Kim MJ, Kim JH, et al. Orphan nuclear receptor Nur77 mediates fasting-induced hepatic fibroblast growth factor 21 expression. Endocrinology. 2014;155:2924–31.
36. Settembre C, De Cegli R, Mansueto G, Saha PK, Vetrini F, Visvikis O, et al. TFEB controls cellular lipid metabolism through a starvation-induced autoregulatory loop. Nat Cell Biol. 2013;15:647–58.

37. Samuel VT, Shulman GI. Nonalcoholic fatty liver disease as a nexus of metabolic and hepatic diseases. Cell Metab. 2018;27:22–41.
38. Brooks SPJ. Chapter 9: Fasting and refeeding: models of changes in metabolic efficiency. In: Storey KB, Storey JM, editors. Cell and Molecular Response to Stress. Amsterdam, Netherlands: Elsevier; 2001:111–27. Available at: https://www.sciencedirect.com/science/article/pii/S1568125401800115?via%3Dihub. Accessed January 1, 2001.
39. Farooq A, Chamari K, Sayegh S, El Akoum M, Al-Mohannadi AS. Ramadan daily intermittent fasting reduces objectively assessed habitual physical activity among adults. BMC Public Health. 2021;21:1912.
40. Minghelli G, Schutz Y, Whitehead R, Jequier E. Seasonal changes in 24-h and basal energy expenditures in rural Gambian men as measured in a respiration chamber. Am J Clin Nutr. 1991;53:14–20.
41. Berndt N, Horger MS, Bulik S, Holzhütter H-G. A multiscale modelling approach to assess the impact of metabolic zonation and microperfusion on the hepatic carbohydrate metabolism. PLOS Comput Biol. 2018;14:e1006005. https://doi.org/10.1371/journal.pcbi.1006005
42. Halpern KB, Shenhav R, Matcovitch-Natan O, Toth B, Lemze D, Golan M, et al. Single-cell spatial reconstruction reveals global division of labour in the mammalian liver. Nature. 2017;542:352–6.
43. Yang J, MacDougall ML, McDowell MT, Xi L, Wei R, Zavadoski WJ, et al. Polyomic profiling reveals significant hepatic metabolic alterations in glucagon-receptor (GCGR) knockout mice: implications on anti-glucagon therapies for diabetes. BMC Genom. 2011;12:281.
44. Benhamouche S, Decaens T, Godard C, Chambrey R, Rickman DS, Moinard C, et al. APC tumor suppressor gene is the "zonation-keeper" of mouse liver. Dev Cell. 2006;10:759–70.
45. Sekine S, Lan BY, Bedolli M, Feng S, Hebrok M. Liver-specific loss of beta-catenin blocks glutamine synthesis pathway activity and cytochrome p450 expression in mice. Hepatology. 2006;43:817–25.
46. Charawi S, Just PA, Savall M, Abitbol S, Traore M, Metzger N, et al. LKB1 signaling is activated in CTNNB1-mutated HCC and positively regulates beta-catenin-dependent CTNNB1-mutated HCC. J Pathol. 2019;247:435–43.
47. Spicer J, Rayter S, Young N, Elliott R, Ashworth A, Smith D. Regulation of the Wnt signalling component PAR1A by the Peutz-Jeghers syndrome kinase LKB1. Oncogene. 2003;22:4752–6.
48. Sun TQ, Lu BW, Feng JJ, Reinhard C, Jan YN, Fantl WJ, et al. PAR-1 is a Dishevelled-associated kinase and a positive regulator of Wnt signalling. Nat Cell Biol. 2001;3:628–36.
49. Zhan YY, Chen Y, Zhang Q, Zhuang JJ, Tian M, Chen HZ, et al. The orphan nuclear receptor Nur77 regulates LKB1 localization and activates AMPK. Nat Chem Biol. 2012;8:897–904.
50. Gougelet A, Torre C, Veber P, Sartor C, Bachelot L, Denechaud PD, et al. T-cell factor 4 and beta-catenin chromatin occupancies pattern zonal liver metabolism in mice. Hepatology. 2014;59:2344–57.

SUPPORTING INFORMATION

Additional supporting information may be found in the online version of the article at the publisher's website.

How to cite this article: Acevedo-Acevedo S, Stefkovich ML, Kang SWS, Cunningham RP, Cultraro CM, Porat-Shliom N. LKB1 acts as a critical brake for the glucagon-mediated fasting response. Hepatol Commun. 2022;6:1949–1961. https://doi.org/10.1002/hep4.1942